ApJL Accepted, March 4th, 2004

OMEGA CENTAURI: THE POPULATION PUZZLE GOES DEEPER[1]

Luigi R. Bedin[2], Giampaolo Piotto[2], Jay Anderson[3], Santi Cassisi[4], Ivan R. King[5], Yazan Momany[2], and Giovanni Carraro[2]

ABSTRACT

We present *HST* observations that show a bifurcation of colors in the middle main sequence of the globular cluster ω Centauri. We see this in three different fields, observed with different cameras and filters. We also present high precision photometry of a central ACS field which shows a number of main-sequence turnoffs and subgiant branches. The double main sequence, the multiple turnoffs and subgiant branches, and other population sequences discovered in the past along the red giant branch of this cluster add up to a fascinating but frustrating puzzle. We suggest various explanations, none of them very conclusive.

Subject headings: globular clusters: individual(NGC 5139) — Hertzsprung-Russell diagram

1. Introduction

A number of properties (total mass, chemical composition, kinematics, and spatial distribution of the stars) make ω Centauri a peculiar object among Galactic globular clusters.

---

[2]Dipartimento di Astronomia, Università di Padova, Vicolo dell'Osservatorio 2, I-35122 Padova, Italy; bedin-piotto-momany-carraro@pd.astro.it

[3]Department of Physics and Astronomy, Mail Stop 108, Rice University, 6100 Main Street, Houston, TX 77005; jay@eeyore.rice.edu

[4]Osservatorio Astronomico di Collurania, via M. Maggini, 64100 Teramo; cassisi@astrte.te.astro.it

[5]Department of Astronomy, University of Washington, Box 351580, Seattle, WA 98195-1580; king@astro.washington.edu

[1]Based on observations with the NASA/ESA *Hubble Space Telescope*, obtained at the Space Telescope Science Institute, which is operated by AURA, Inc., under NASA contract NAS 5-26555.

The most evident anomaly is the large spread in metallicity seen both in spectroscopic (Norris & Da Costa 1995) and photometric (Hilker & Richtler 2000, Lee et al. 1999, Pancino et al. 2000) investigations.

Most of the fascinating results on ω Cen come from the evolved stellar population, which can be studied in detail from the ground. In this paper we use *HST* data to explore the cluster's turnoff (TO) and main-sequence (MS) populations. While studies of the evolved red giant branch (RGB) can explore metallicity, kinematic, and spatial-distribution issues, we need the fainter stars if we hope to learn anything about ages and mass functions, and to give us better statistics (there are $\sim$10 MS stars for every RGB star).

The present paper was stimulated by preliminary results by one of us (Anderson 1997, 2002, 2003), on the presence of multiple turnoffs and of a bifurcated main sequence (MS). Here we confirm that the unusual features found in the color-magnitude diagrams are not some data-reduction artifact, or a local phenomenon. The features are real and are present throughout the cluster. Unfortunately, the striking results we present here lead to more questions than they answer. Though it will take a lot of time to fully exploit the ω Cen data stored in the *HST* archive (and we are working on this), we think that these new results are worthy of immediate publication because of their importance to the ongoing debate on the nature of this object.

2. Observations and Data Reduction

In this paper we use WFPC2 and ACS *HST* data to construct color–magnitude diagrams (CMDs) which extend from 1–2 magnitudes above the TO to more than 7 magnitudes below it. In particular, we have used the following sets of images: 1) GO 9444 (ACS/WFC): 4×1350s F814W and 4×1350s F606W; 2) GO 9442 (ACS/WFC): 27×340s F435W and 36×440s F658N (a 3×3 mosaic at the center); 3) GO 6821 (WFPC2): 2×1s, 2×10s, 8×100s in F675W, and 26s, 2×260s in F336W; 4) GO 5370 (WFPC2): 2×300s, 600s F606W, and 2×400s, 1000s in F814W. All these images have been reduced with the algorithms described in Anderson & King (2000). Photometric calibration has been done according to the Holtzman et al. (1995) flight system for the WFPC2 data; for ACS/WFC we used the preliminary Vega System zero points available on the ACS website.

3. The color–magnitude diagram: observational evidence

The left part of Figure 1 shows four CMDs: the two upper panels focus on the turnoff region, and the lower ones on the main-sequence region. Panel a shows the original WFPC2 CMD that first discovered the lower turnoff (LTO) sequence (Anderson 2003). Panel b shows the same sequence (from WFC data) with many more details and more stars, from a larger region of the cluster. There are a number of distinct TOs and subgiant branches (SGBs), and the connection of the LTO to the metal-rich red giant branch (called RGB-a by Pancino et al. 2000) can be seen more clearly with more stars. We show Hα photometry here instead of R_{625} because there are more exposures and we can therefore make a better estimate of the photometric errors.

Ferraro et al. (2004) reduced the same ACS field in their recent study of the LTO population. They made the obvious association that this LTO corresponds to the metal-rich ([Fe/H] ~ -0.5) RGB-a population, and found that it could be fit only with an old (15 Gyr) isochrone. They found little or no age difference between the metal-rich and metal-poor populations. In our diagram, it is clear that not only is there a lower subgiant branch, but we can also see the lower turnoff at a color that is clearly redward of the main population sequence. We also see several SGBs: the LTO SGB, a distinct SGB at the bright end of the main population, and some distinct structure in the region between the upper and lower SGB. Clearly, this is telling us a lot about the cluster's populations, but the interpretation is complicated by age, metallicity, and distance degeneracies. We will confine the focus of this letter to the populations farther down the main-sequence, deferring a detailed analysis of the turnoff population to when all the WFC central data have been reduced and some information on the metallicity of the different TO-SGBs will be available.

Surely the most intriguing feature in the CMDs of Fig. 1 is the double main sequence (DMS), which is clearly visible in the bottom two panels (c, d). Panel c shows the original V_{606} vs. $V_{606} - I_{814}$ WFPC2 CMD from Anderson (1997, 2002), where the DMS was first identified. Not only is the main sequence much broader than photometric errors, it appears to bifurcate into two distinct sequences, with a region between the two that is almost devoid of stars. Panel d shows a new V_{606} vs. $V_{606} - I_{814}$ CMD from ACS/WFC images, which also shows the anomalous DMS in a different field, at $17'$ from the center. The DMS can even be discerned in the very inner part of the cluster (panels b and e).

We have CMDs from different fields, observed with two different cameras, in different photometric bands. The anomalous DMS is present in all four (panels b, c, d, e). There can be no doubt that the double sequence is a real and ubiquitous feature in ω Cen.

If we were to guess what the main sequence should look like from our knowledge of the stars on the giant branch, we would expect a sequence about 0.03 mag in width, with a concentration to a blue edge, corresponding to the metal-poor (MP) population containing about 65% of the stars, a tail to the red corresponding to the intermediate-metallicity (Mint) population containing about 30% of the stars, and a small even redder component from the metal-rich RGB-a population with 5% of the stars (we adopt the population labels from Pancino et al. 2000). The sequence we observe here could not be more different from these expectations.

Let us take note of a few simple facts from Fig. 1: (1) The two sequences are clearly separated, at least in the interval $22 < V_{606} < 20.5$, with a region almost devoid of stars between them. (2) The bluer MS (bMS) is much less populous than the red MS (rMS). The bMS contains 25% to 35% of the stars. (3) The DMS extends down to at least $V_{606} \sim 23.5$. Below this, the bMS appears to vanish, though it is difficult to say for sure if it peters out, or if it blends with the rMS as the photometric errors increase. (4) Finally we note that panels b and e show clearly that the bMS is a different population from the LTO–RGB-a population.

The DMS that we observe represents a real puzzle for at least two reasons. First, the bifurcation itself is puzzling. As summarized above, the many detailed photometric and spectroscopic investigations of the RGB indicate a spread of metallicities, not two distinct populations. The only truly distinct population seen is the metal-rich component. Second, the less populous of our two MSs is the blue one. This is even more difficult to understand. Assuming that all the stars in the two MSs are members of ω Cen, any canonical stellar models with canonical chemical abundances tell us that the bMS *must* be more metal poor than the rMS. However, both spectroscopic (Norris & Da Costa 1995) and photometric (e.g., Hilker & Richtler 2000) investigations show that the distribution in metallicity of the ω Cen stars begins with a peak at $[\mathrm{Fe/H}] \sim -1.6$, and then tails off on the metal-rich side.

4. Comparison with theoretical models

The previous section has confronted us with several seemingly contradictory observational facts concerning the CMD and populations of ω Cen. In this section we will see what light stellar models can shed on the situation. Because the ACS photometric system is not yet adequately calibrated, we will confine our isochrone-fitting analysis to the WFPC2 data. The adopted stellar models are an extension of the updated evolutionary models for very-low-mass stars and more massive ones presented by Cassisi et al. (1999, 2000). All models and isochrones have been transformed into the WFPC2 observational planes by using the accurate bolometric corrections kindly provided to us by F. Allard (see also Allard et al.

1997).

In fitting the stellar models we have adopted a reddening $E(B-V) = 0.13$ and a distance modulus $(m-M)_0 = 13.6$. We used the absorption coefficients for the WFPC2 bands listed in Table 12b of Holtzman et al. (1995). For the F606W band we adopted a mean of the absorption coefficients in F555W and F675W. In Figure 2a and 2c we have overplotted 4 sets of isochrones, corresponding to metallicities from [Fe/H] = −2.1 to −0.6, which covers the entire metallicity range of the stellar population of ω Cen (Norris & Da Costa 1995), and corresponding to an age of 14 Gyr.

Since we are able to see the actual turnoff and not just the SGB (as in Ferraro et al. 2004), and since we use a $U-R$ CMD, we are more sensitive to the population's metallicity. Panel a of Fig. 2 shows that a more metal-poor isochrone would fit the LTO better. Indeed, Origlia et al. (2003) have shown that the RGB-a stars have a metallicity in the interval $-0.9 <$ [Fe/H] < -0.5. It does appear that the LTO population would be fit with a metallicity near the middle of this range.

Panel b of Fig. 2 shows the cluster main sequence in the F606W vs. F606W−F814W bands, along with isochrones for the cluster's metallicity range. There are several features worth noting: first, the [Fe/H] = −1.6 isochrone clearly follows along the rMS. Second, canonical models are not able to explain the bMS. In order to explain the 0.06 mag $V-I$ color difference between the two sequences at $V \sim 21$, we would have to assume that the bMS stars are extremely metal-poor ([Fe/H] $\ll -2.0$), though it would seem absurd to have such a large population of low-metallicity MS stars when there is no evidence whatever for such stars along the much-studied RGB. The only way to force the model to fit the two sequences with the metallicity spread seen in the RGB would be to shift the models arbitrarily in color and/or magnitude.

We can imagine four possible explanations, though we admit that all of them seem far-fetched. (1) The models or calibrations are grossly in error *and* the distribution of metallicities is vastly different for the RGB stars than for the MS stars. (2) The bMS represents some super-metal-poor population ([Fe/H] $\ll -2.0$). (3) The bMS represents a super-helium-rich ($Y \geq 0.3$) population. (4) The bMS represents a population of stars about 1–2 kpc behind ω Cen. We examine these four possibilities in the following section.

5. Discussion

One way to interpret the observations is to assume that either the photometric calibration or the isochrones are in error. If the net error is 0.06 mag in $V-I$ color, then perhaps the metal-poor (MP) population ([Fe/H] $=-1.6$) follows along the bMS instead of along the rMS. If this is the case then the rMS would correspond to the metal-rich population ([Fe/H] $=-0.5$), as the 0.06 mag $V-I$ separation cannot be explained by the metallicity difference between the MP and Mint populations. (While it may be conceivable that the isochrones could have errors in an absolute sense, they should be reliable in a differential sense.) There are additional problems with this interpretation. First is that only 5% of the RGB stars are metal rich, but in this scenario over 70% of the MS stars would be metal rich. This would imply drastically different mass functions, such as have never been seen before anywhere (see Piotto & Zoccali 1999). Furthermore, there is no actual gap in the observed metallicity distribution and in the color distribution of the RGBs of the MP and Mint populations. Most importantly, the fact that the MS extension of the LTO runs parallel to the rMS (on the red side of it, panel e) makes this scenario impossible.

The second interpretation is that the rMS corresponds to the MP stars, but the bMS corresponds to a super-metal-poor population, with [Fe/H] $\ll -2$. However, such a large population of metal-poor stars has never been observed in ω Cen or in any other globular.

The third possibility is that the populations of the two MSs have sensibly different helium content (Y). Norris, Freeman, & Mighell (1996) have shown that the metallicity distribution of ω Cen stars can be well fitted by two separate components, and argued that this can be explained by two successive epochs of star formation. Assuming for the more metal-rich ([Fe/H] $=-1.0$) Mint population a helium content of $Y \sim 0.30$, we find that the corresponding MS would be ~ 0.07 magnitude bluer in $(V-I)$ than the MP MS (assumed to have a canonical $Y = 0.23$, and [Fe/H] $=-1.6$). Note that Norris et al. (1996) found that the ratio of the Mint to MP population should be 0.2, compatible, within the uncertainties, with the value we find for the rMS/bMS ratio. Panel e of Fig. 1 shows that the bMS could well be connected with the intermediate TO-SGB. Panel a of Fig. 2 shows that this intermediate SGB is slightly brighter than the luminosity expected for a metallicity similar to the Mint, and the expected TO is redder than the observed one. These observational facts are consistent with this population beeing helium enhanced and slightly younger, as expected if the helium enhancement is due to self-pollution from intermediate AGB MP stars. The dramatic increase of s-process heavy-element abundances with metallicity found by Smith et al. (2000) in ω Cen RGB stars furtherly support the hypothesis that Mint stars could have formed from material polluted by ejecta from 1.5-3 $m_\odot$ AGB stars. The presence of a population with high helium content could also account for the anomalously hot HB of ω Cen, following the calculations of D'Antona et al. (2002). All this notwithstanding, a $Y \geq 0.30$ is higher than any value so far measured in Galactic GCs (Salaris et al. 2004), and not easy to understand.

As a fourth possibility, if we assume that the rMS corresponds to the majority of the cluster stars, the bMS could correspond to a population of stars located behind ω Cen. As shown in panel d of Fig. 2, if the bMS is populated by stars located 1.6 kpc beyond ω Cen, we can easily fit it with an [Fe/H] = -1 isochrone. Panel e of Fig. 1 appears to strengthen this hypothesis: we see the bMS get closer and closer to the rMS, crossing it at $H\alpha \sim 18.5$, and apparently continuing into a broadened TO and SGB. This broadening of the intermediate TO could be the result of a spread in both metallicity and distance. The overall appearance of the CMD is that there are two sequences, shifted by up to $\sim$ 0.3–0.5 magnitude. The hypothesis of a background agglomerate of stars with metallicity around [Fe/H] ~ -1.0 would also naturally explain why the bMS appears to intersect the rMS at $V_{606} \sim 23.5$ (cf. Figs. 1c and 1d). Such a background object would naturally explain the observation that the giants of different metallicity appear to have somewhat different spatial distributions (Jurcsik 1998, Hilker & Richtler 2000), though this spatial variation could be explained by merger or self-enrichment scenarios as well.

Leon, Meylan, & Combes (2000) have identified a tidal tail around ω Cen. Tidal tails often have a clumpy nature. However, the number of stars in the bMS seems to be too large and the sequence too sharp to be interpreted as a part of a clump in a tidal tail behind the cluster. Another possibility is that the object in the background is a distinct cluster or a dwarf galaxy. As it should cover at least 20–30 arcmin in the sky (this is the extent of the region where we identified a DMS) and be located at about 7 kpc from the Sun, the object should be extended by at least 40–60 pc. The probability of observing such an object in the direction of ω Cen is extremely low. However, if this object happens to be gravitationally linked to ω Cen (either because it was part of the same original system or because it is the remnant of some merging event), that would enhance the probability of seeing it in the same direction as ω Cen.

We note that the idea of a population of stars behind the cluster has been suggested before. Ferraro et al. (2002) measured a bulk motion for the RGB-a stars with respect to the other cluster stars, and interpreted this as evidence that it could be a background object, or a merger product that has not yet phase-mixed. However, Platais et al. (2003) find this motion spurious, attributing it to a color/magnitude term in the proper motions. Moreover, Anderson (2003), using very accurate WFPC2 proper motions, contradicts the bulk motions seen by Ferraro et al. (see his Fig. 1). In any case, the background population we consider here could not correspond to the very metal-rich population; our Fig. 1e makes it clear that the LTO and the bMS are not related to each other.

6. Resolving the controversy

Much of the current puzzle stems from our inability to interrelate the various RGB, SGB, TO, and MS populations. Currently there exists a good data base of observations for RGB stars, but only spot observations of the SGB, TO, and MS populations. An accurate analysis of the proper-motion, radial-velocity, metallicity, and spatial distributions of the MS, TO, SGB stars of ω Cen, in a large field sampled over the inner 20 arcmin or so of the cluster, along with detailed theoretical calculations, are absolutely essential to explain the observational facts, which at the moment represent a mixed-up puzzle. The new results presented in this paper show that the more we learn about this cluster, the more we realize we do not know.

We thank the referee, John Norris, and Raffaele Gratton for useful suggestions and discussions on the role of helium in interpreting the observations presented in this paper. L.R.B., G.C., S.C., Y.M., and G.P. acknowledge financial support by MIUR (PRIN2001, PRIN2002, and PRIN2003). J.A. and I.R.K. acknowledge support by STScI grant GO 9444.

REFERENCES

Allard, F., Hauschildt, P. H., Alexander, D. R., & Starrfield, S. 1997, ARA&A, 35, 137

Anderson, J. 1997, PhD Thesis, UC, Berkeley

Anderson, J., & King, I. R. 2000, PASP, 112, 1360

Anderson, J. 2002, in ASP Conf. Ser. 265, *"ω Centauri a Unique Window into Astrophysics"*, ed. F. van Leeuwen, J. Hughes, & G. Piotto (San Francisco: ASP), 87

Anderson, J. 2003, in ASP Conf. Ser. 296, *"New Horizons in Globular Clusters Astronomy"*, ed. G. Piotto, G. Meylan, S. G. Djorgovski, & M. Riello (San Francisco: ASP), 125

Cassisi, S., Castellani, V., Ciarcelluti, P., Piotto, G., & Zoccali, M. 2000, MNRAS, 315, 679

Cassisi, S., Castellani, V., Degl'Innocenti, S., Salaris, M., & Weiss, A. 1999, A&AS, 134, 103

D'Antona, F., Caloi, V., Montalbán, J., Ventura, P., & Gratton, R. 2002, A&A, 395, 69

Ferraro, F. R., Bellazzini, M., & Pancino E. 2002, ApJ, 573, L95

Ferraro, F. R., Sollima, A., Pancino E., Bellazzini, M., Straniero, O., Origlia, L., & Cool, A. M. 2004, preprint (astro-ph/0401540)

Hilker, M., & Richtler, T. 2000, A&A, 362, 895

Holtzman, J. A., Burrows, C. J., Casertano, S., Hester, J. J., Trauger, J. T., Watson, A. M., & Worthey, G. 1995, PASP, 107, 1065

Jurcsik, J. 1998, ApJ, 506, L113

Lee, Y. W., Joo, J. M., Sohn, Y. J., Rey, S. C., Lee, H. C., & Walker, A. R. 1999, Nature, 402, 55

Leon, S., Meylan, G., & Combes, F. 2000, A&A, 359, 907

Norris, J. E., & Da Costa, G. S. 1995, ApJ, 447, 680

Norris, J. E., Freeman, K. C., & Mighell, K. J. 1996, ApJ, 462, 241

Origlia, L., Ferraro, F. R., Bellazzini, M., & Pancino, E. 2003, ApJ, 591, 916

Pancino, E., Ferraro, F. R., Bellazzini, M., Piotto, G., & Zoccali, M. 2000, ApJ, 534, L83

Piotto, G., & Zoccali, M. 1999, A&A, 345, 485

Platais, I., Wyse, R. F. G., Hebb, L., Lee, Y. W., & Rey, S. C. 2003, ApJ, 591, L130

Salaris, M., Riello, M., Cassisi, S., & Piotto, G. 2004, A&A, subm.

Smith, V. V., Suntzeff, N. B., Cunha, K., Gallino, R., Busso, M., Lambert, D. L., & Straniero, O., AJ, 119, 1239.

This preprint was prepared with the AAS LATEX macros v5.2.

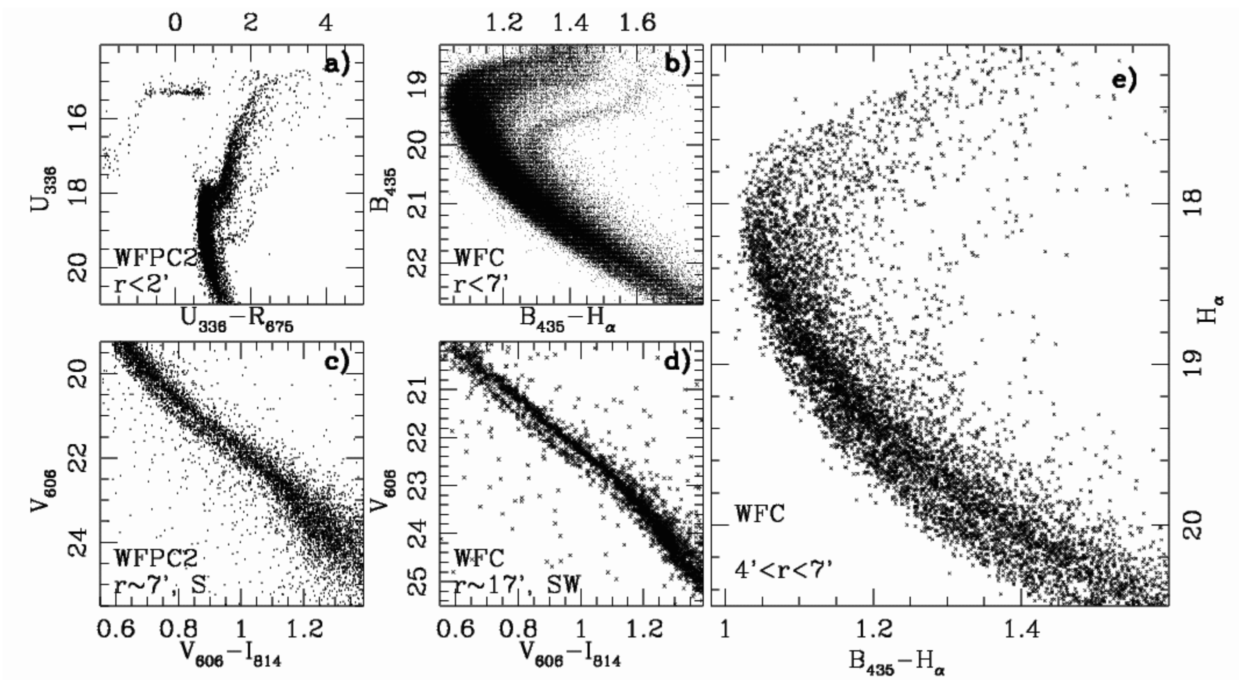

Fig. 1.— A collection of CMDs from WFPC2 and ACS data of ω Cen. For each CMD, the label indicates the distances of the field from the cluster center. Panel e shows the subsample of the stars plotted in panel b, located at radial distances r> $4'$ and with photometric rms lower than 0.025 magnitudes.

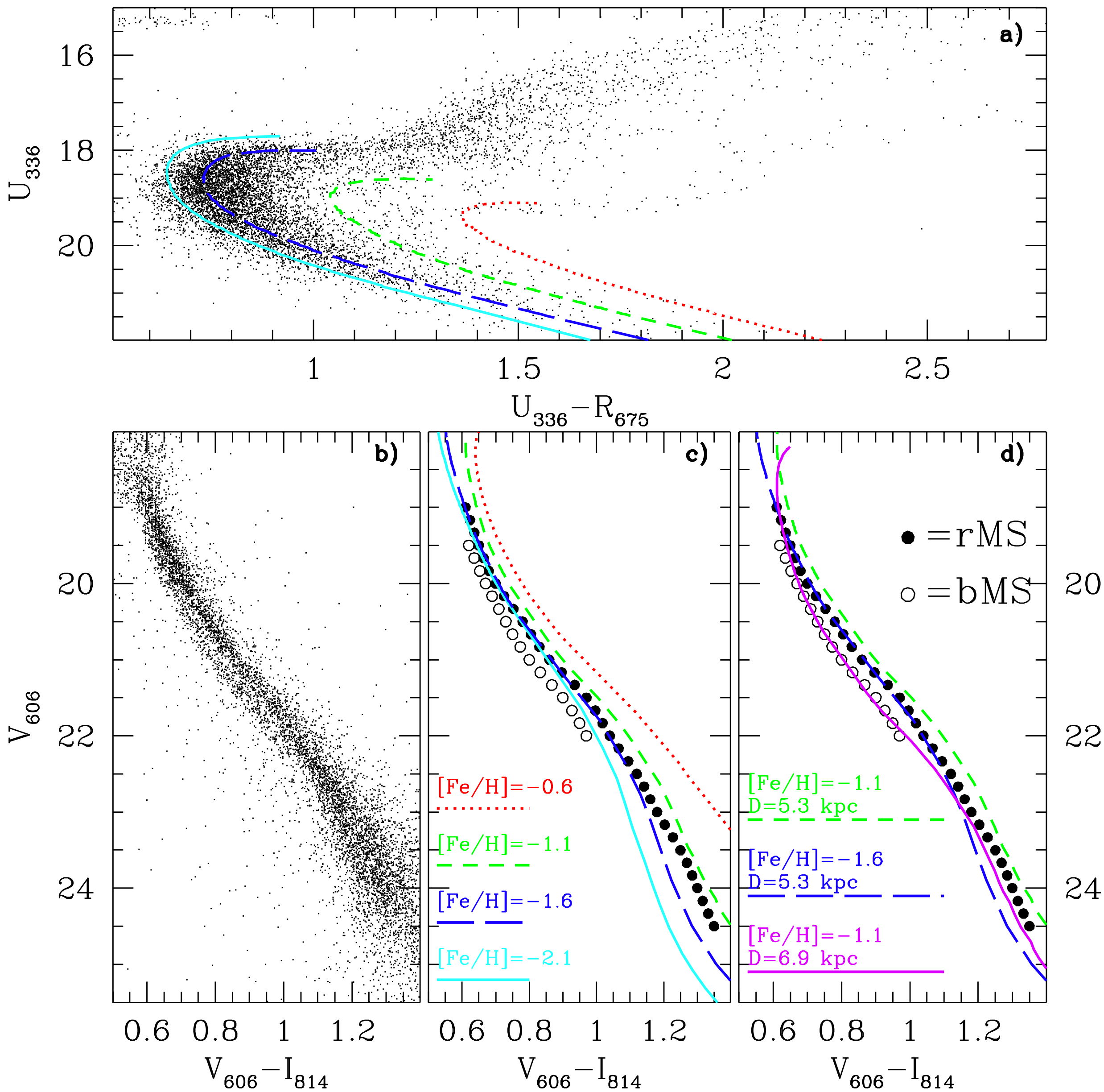

Fig. 2.— Comparison of theoretical models with WFPC2 observations of the TO region (panel a), and the DMS adopting the same distance (as in panel a) for all the isochrones (panel c), and shifting the [Fe/H] = −1.1 isochrone by 1.6 kpc (panel d). For clarity we have plotted only the fiducial points of the rMS and the bMS.